Journal of Solid State Chemistry **145,** 705–710 (1999)
Article ID jssc.1999.8290, available online at http://www.idealibrary.com on IDEAL®

Crystal Structures and Magnetic Properties of $Ca_{2-x}Sr_xMnO_4$

Keitaro Tezuka, Masaaki Inamura, and Yukio Hinatsu

Division of Chemistry, Graduate School of Science, Hokkaido University, Sapporo 060-0810, Japan

and

Yutaka Shimojo and Yukio Morii

Japan Atomic Energy Research Institute, Tokai-mura, Ibaraki 319-1195, Japan

Received December 7, 1998; in revised form March 12, 1999; accepted March 23, 1999

We prepared Ruddlesden–Popper-type layered perovskites $Ca_{2-x}Sr_xMnO_4$ ($x = 0$–2.0 at 0.25 intervals). Their precise crystal structures at room temperature and at 10 K were determined from both the X-ray and the neutron diffraction measurements. The compounds for $x = 0$ and 0.25 have a tetragonal system with the space group $I4_1/acd$ (No. 142). The compounds for $x = 0.5$–2.0 have a tetragonal system with the space group $I4/mmm$ (No. 139). Magnetic susceptibility measurements have been performed for all the compounds in the temperature range between 5 and 350 K. The temperature-dependent magnetic susceptibilities were measured under zero-field-cooled (ZFC) and field-cooled (FC) conditions at an applied field of 1000 G. A dramatic difference in magnetic susceptibilities between ZFC and FC was observed below the Néel temperatures for Ca_2MnO_4 and $Ca_{1.75}Sr_{0.25}MnO_4$, which shows the onset of a ferromagnetic moment below these temperatures. This moment is caused by the Dzyaloshinsky–Moriya interaction. Magnetic structures of $Ca_{2-x}Sr_xMnO_4$ ($x = 0.0$, 0.5, 1.0, and 1.5) solid solutions at 10 K have been determined by the neutron diffraction measurements. The nearest-neighbor Mn^{4+} ions are coupled antiferromagnetically in the (001) planes and the spins are parallel to the c axis.

INTRODUCTION

In the SrO and MnO_2 system, β-Sr_2MnO_4 is a higher temperatures phase existing above 1873 K. This compound has a layered perovskite-type structure with the space group $I4/mmm$ (No. 139); i.e., it has an ideal Ruddlesden–Popper-type structure (K_2NiF_4-type structure). It shows an antiferromagnetic transition at ca. 170 K, which has been turned out by the powder neutron diffraction experiment. The transition was not determined by the magnetic susceptibility measurement because its magnetic interaction has a strong two dimensionality (1).

Ca_2MnO_4 also has a layered perovskite structure. However, it does not have an ideal Ruddlesden–Popper-type structure; i.e., the octahedra MnO_6 of the compound rotate slightly around the c axis from an ideal Ruddlesden–Popper-type structure with the space group $I4/mmm$. As a result, it takes a tetragonal unit cell with the space group $I4_1/acd$, and its unit cell is related to the K_2NiF_4-type unit cell in the following way: $a = \sqrt{2}a'$ and $c = 2c'$ (where a' and c' are the lattice parameters for the K_2NiF_4-type unit cell) (2).

Ca_2MnO_4 shows an unusual magnetic susceptibility behavior, with a very shallow maximum around 220 K and a fairly sharp peak at 114 K (3, 4). A powder neutron diffraction study of this compound has revealed that three-dimensional ordering sets in at 114 K with an antiferromagnetic structure different from that of K_2NiF_4 (3).

Since the crystal structures of these two compounds are similar, the formation of solid solutions $Ca_{2-x}Sr_xMnO_4$ is expected over a wide range of x. Through magnetic studies on these solid solutions, we may obtain information on the nature of the large difference found in the magnetic susceptibility vs temperature curves for Ca_2MnO_4 and β-Sr_2MnO_4, and the relationship between the crystal structure and magnetic properties for these Ruddlesden–Popper-type compounds. In this study, we have prepared solid solutions $Ca_{2-x}Sr_xMnO_4$ and have performed their detailed crystallographic and magnetic structure studies, using not only magnetic susceptibility measurements but also X-ray and neutron diffraction measurements. We will discuss their results.

EXPERIMENTAL

Solid solutions $Ca_{2-x}Sr_xMnO_4$ ($x = 0$–2.0 at 0.25 interval) were prepared by the standard solid-state reaction. Starting materials were $CaCO_3$ or $SrCO_3$ and MnO_2, which were dried in advance at 423 K before use. They were

0022-4596/99 $30.00

ground in an agate mortar, pressed into pellets, and heated in a flow of oxygen gas at 1573 K for 24 h. After cooling, they were reground, repressed into pellets, and heated in a flow of oxygen gas at 1573 K for 48 h. Since the samples with $x \geq 0.5$ are an α phase having a crystal structure different from the Ruddlesden–Popper-type structure, these samples were refired in air at 1773 K ($x = 0.5$ and 0.75), 1823 K ($x = 1.0$), 1873 K ($x = 1.25$ and 1.5), or 1923 K ($x = 1.75$ and 2.0) for 30 min in order to change the α phase into a higher temperature phase (β phase) with a K_2NiF_4-type structure and were then rapidly cooled in air.

Powder X-ray diffraction patterns were measured with Cu$K\alpha$ radiation on a Rigaku RINT2000 diffractometer. The structures were refined with the Rietveld analysis method, using the program Rietan (5).

Powder neutron diffraction profiles were measured for $x = 0$, 0.5, 1.0, and 1.5 with a high-resolution powder diffractometer (HRPD) in the JRR-3M reactor (Japan Atomic Energy Research Institute), with a Ge(331) monochromator ($\lambda = 1.823$ Å). The collimators used were 6′–20′–6′, which were placed before and after the monochromator and between the sample and each detector. The set of 64 detectors and collimators, which were placed every 2.5°, rotate around the sample. The measurements were made at 10 K and room temperature.

Magnetic susceptibilities were measured with a SQUID magnetometer (Quantum Design, MPMS model) after zero-field-cooling (ZFC) and field-cooling (FC) processes in the temperature range 5–350 K. The external magnetic field applied was 1000 G. The remnant magnetization measurements were also performed. The samples were cooled to 5 K in a zero field. The magnetic field was applied up to 50,000 G and then reduced to zero, and the magnetization measurements were performed in the temperature range from 5 to 350 K. The field dependence of the magnetization was measured at 10 K by changing the magnetic field strength in the range between −5000 and 5000 G.

RESULTS AND DISCUSSION

Crystal Structure

The $Ca_{2-x}Sr_xMnO_4$ systems form a solid solution phase with a tetragonal-layered perovskite structure (Ruddlesden–Popper-type A_2BO_4) over a range of $0 \leq x \leq 2$. Their X-ray diffraction profiles at room temperature were indexed with a tetragonal unit cell, space group $I4_1/acd$ (No. 142) for $x = 0$–0.25, and $I4/mmm$ (No. 139) for $x = 0.5$–2.0, as shown in Fig. 1; i.e., $Ca_{2-x}Sr_xMnO_4$ for $x = 0.5$–2.0 were determined to have the ideal Ruddlesden–Popper-type structure. Ca_2MnO_4 and $Ca_{1.75}Sr_{0.25}MnO_4$ have a more complex crystal structure and the octahedra MnO_6 rotate around the c axis. The rotation scheme is shown in Fig. 2. The rotation of the octahedra MnO_6 causes superlattice reflections (21l), l odd, and (41l), l odd: the space group of these compounds is

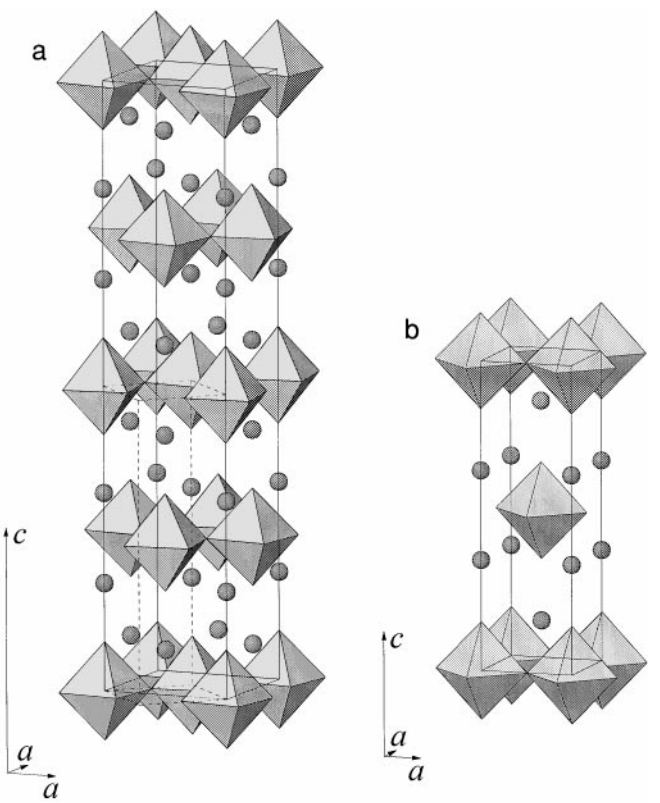

FIG. 1. Crystal structures of $Ca_{2-x}Sr_xMnO_4$: (a) a tetragonal structure with space group $I4_1/acd$ ($x = 0$ and 0.25) and (b) a tetragonal structure with space group $I4/mmm$ ($x = 0.5 \sim 2.0$).

$I4_1/acd$. The unit cell (a, c) is related to the K_2NiF_4-type unit cell (a', c') in the following way: $a = \sqrt{2}a'$; $c = 2c'$. A similar structural distortion has been observed in Sr_2IrO_4 (6). The

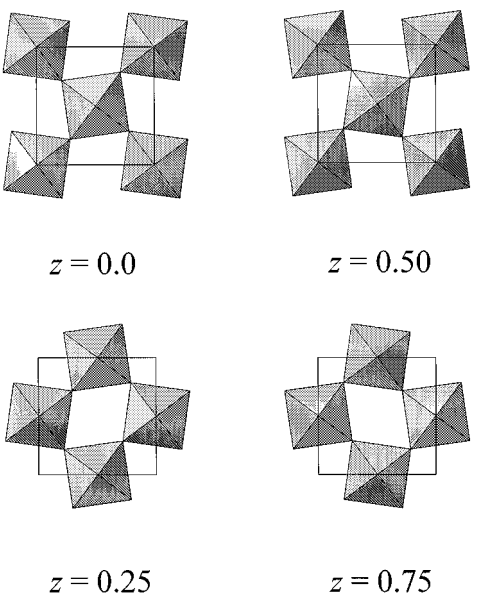

FIG. 2. Rotation scheme of MnO_6 octahedra for space group $I4_1/acd$.

TABLE 1
Crystallographic Information for $Ca_{2-x}Sr_xMnO_4$ from X-Ray Diffraction Measurements

x	0	0.25	0.5	1.0	1.5	2.0
Space group	$I4_1/acd$	$I4_1/acd$	$I4/mmm$	$I4/mmm$	$I4/mmm$	$I4/mmm$
a/Å	5.1890(1)	5.2160(1)	3.7099(1)	3.7446(1)	3.7714(1)	3.8022(2)
c/Å	24.130(1)	24.216(1)	12.134(1)	12.224(1)	12.366(1)	12.519(1)
Ca, Sr						
z	0.175(1)	0.176(1)	0.354(1)	0.355(1)	0.355(1)	0.355(1)
B/Å^2	0.69	0.70	0.66	0.68	0.66	0.65
Mn						
B/Å^2	0.25	0.33	0.31	0.27	0.25	0.30
O1						
z	0.080(1)	0.080(1)	0.0	0.0	0.0	0.0
B/Å^2	0.98	0.79	0.92	0.84	1.02	0.90
O2						
x	0.213(2)	0.218(3)	0.0	0.0	0.0	0.0
z	0.25	0.25	0.159(2)	0.161(2)	0.157(3)	0.156(1)
B/Å^2	1.17	1.56	0.99	1.14	1.53	1.26
R_{wp}	12.74	11.71	10.09	9.88	10.09	13.93

Note. The structure was refined in the tetragonal space groups $I4_1/acd$ and $I4/mmm$. The four unique atoms have the following positions: for $I4_1/acd$, (Ca, Sr) (0.0, 0.0, z), Mn (0.0, 0.0, 0.0), O1 (0.0, 0.0, z), and O2 (x, x, 0.25); for $I4/mmm$, (Ca, Sr) (0.0, 0.0, z), Mn (0.0, 0.0, 0.0), O1 (0.0, 0.5, 0.0), and O2 (0.0, 0.0, z).

results of the Rietveld analysis are shown in Table 1. With increasing Sr concentration in the $Ca_{2-x}Sr_xMnO_4$ solid solutions, the lattice parameter c becomes larger as shown in Fig. 3; i.e., the distance between the MnO_6 octahedron layers becomes larger.

Neutron diffraction measurements were also performed for $Ca_{2-x}Sr_xMnO_4$ ($x = 0.0$, 0.5, 1.0, and 1.5) both at room temperature and at 10 K, to determine their precise crystal structures and magnetic structures at low temperatures. The results were analyzed with the Rietveld method, and they are shown in Table 2. The results of $Ca_{2-x}Sr_xMnO_4$ by the neutron diffraction measurements at room temperature agree well with those by the X-ray diffraction measurements. The crystal structures of $Ca_{2-x}Sr_xMnO_4$ at 10 K have the same results as those at room temperature and the cell volumes at 10 K are smaller than those at room temperature.

Magnetic Properties

A. Magnetic susceptibility. Temperature dependence of the magnetic susceptibilities for the $Ca_{2-x}Sr_xMnO_4$ is shown in Fig. 4. Ca_2MnO_4 shows clearly the paramagnetic-to-antiferromagnetic transition at 113 K, which is the same as the result reported previously (4). With increasing Sr concentration in the $Ca_{2-x}Sr_xMnO_4$ solid solutions, the peak of the magnetic transition at ca. 110 K becomes ambiguous in the magnetic susceptibility vs temperature curves, and it vanishes completely in the Sr_2MnO_4. This result indicates that, with increasing Sr concentration, the characteristic of the magnetic interaction between the Mn^{4+} ions becomes two-dimensional; i.e., the interlayer magnetic interaction decreases. With increasing Sr concentration in $Ca_{2-x}Sr_xMnO_4$, the distance between the layers becomes larger as described above, which is consistent with the results by the magnetic susceptibility measurements.

In the magnetic susceptibilities for Ca_2MnO_4 and $Ca_{1.75}Sr_{0.25}MnO_4$, dramatic differences between their ZFC and FC susceptibilities are observed below their Néel temperatures. These results suggest that the magnetic moments of Mn^{4+} ions in these two compounds order with a slight ferromagnetic component below Néel temperatures.

To study the existence of the ferromagnetic moment, the measurements of the remnant magnetization and the magnetization vs magnetic field curve (the magnetic hysteresis loop) were performed for all the compounds. Figure 5 shows that the remnant magnetization (weak ferromagnetic moments) observed for both Ca_2MnO_4 and $Ca_{1.75}Sr_{0.25}MnO_4$ disappears above Néel temperatures; i.e., it has been confirmed that the magnetic moments of Mn^{4+} ions showing antiferromagnetic interactions have the weak ferromagnetic component below the Néel temperatures. A small magnetic hysteresis has also been found at 10 K only for Ca_2MnO_4 and $Ca_{1.75}Sr_{0.25}MnO_4$, which means that there exists a ferromagnetic component in the magnetic moment of manganese. It is calculated to be ca. 10^{-4} μ_B/Mn for both samples from the magnetic hysteresis curve.

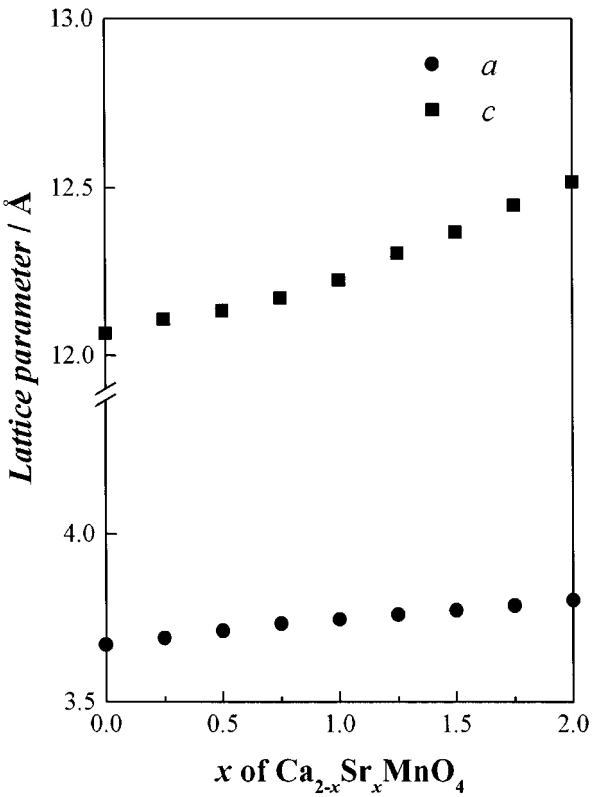

FIG. 3. Lattice parameters for $Ca_{2-x}Sr_xMnO_4$. For space group $I4_1/acd$, the lattice parameters a and c are shown as $a = a(\text{real})/\sqrt{2}$ and $c(\text{real})/2$, respectively.

In the case of Ca_2MnO_4 and $Ca_{1.75}Sr_{0.25}MnO_4$ with the space group $I4_1/acd$, the octahedra MnO_6 rotate around the c axis from the ideal Ruddlesden–Popper-type structure with the space group $I4/mmm$, as shown in Figs. 1 and 2. Inversion symmetry disappears at the center between manganeses. Therefore, the Dzyaloshinsky–Moriya interaction should exist between the magnetically ordered elements at 8*a* sites, from the point of crystalline symmetry. The present experimental results that these two compounds have the weak ferromagnetic component are consistent with this theory.

B. Magnetic structure. In the powder neutron diffraction profiles measured at 10 K, magnetic Bragg peaks are present for all compounds.

We will consider the magnetic structures for $Ca_{2-x}Sr_xMnO_4$ ($x = 0, 0.5, 1.0$, and 1.5) at 10 K. The crystal structure of Ca_2MnO_4 at this temperature is tetragonal with the space group $I4_1/acd$ and the magnetic Bragg peaks can be indexed in the crystallographic unit cell. The space group of the other solid solutions is $I4/mmm$ and magnetic Bragg peaks are indexed in the magnetic unit cell, $a_{mag} = 2a_{cry}$ and $c_{mag} = c_{cry}$. The direction of the magnetic moment for all the compounds has been decided to be parallel to the z axis, and their magnetic structures are shown in Fig. 6.

The magnetic moments of the Mn^{4+} ion at 10 K (shown in Table 2) are much smaller than those expected for a $3d^3$ ion (it is calculated to be 3.87 μ_B). This difference is probably due to the zero-point spin deviation effect and to the strong

TABLE 2
Crystallographic Information for $Ca_{2-x}Sr_xMnO_4$ from Neutron Diffraction Measurements

x	0	0.5	1.0	1.5
		Room temperature		
Space group	$I4_1/acd$	$I4/mmm$	$I4/mmm$	$I4/mmm$
a/Å	5.1900(2)	3.7117(1)	3.7458(3)	3.7742(1)
c/Å	24.141(1)	12.139(1)	12.235(1)	12.403(1)
Ca, Sr				
z	0.176(1)	0.354(2)	0.353(2)	0.355(1)
B/Å^2	0.73	0.65	0.71	0.63
Mn				
B/Å^2	0.34	0.41	0.32	0.52
O1				
z	0.081(1)	0.0	0.0	0.0
B/Å^2	0.81	1.20	0.98	1.27
O2				
x	0.219(2)	0.0	0.0	0.0
z	0.25	0.161(2)	0.156(3)	0.157(2)
B/Å^2	1.40	1.41	1.04	0.94
R_{wp}	17.35	12.81	14.28	13.16
		10 K		
Space group	$I4_1/acd$	$I4/mmm$	$I4/mmm$	$I4/mmm$
a/Å	5.1707(3)	3.6990(1)	3.7344(1)	3.7634(1)
c/Å	24.130(1)	12.142(1)	12.226(1)	12.391(1)
Ca, Sr				
z	0.176(1)	0.353(1)	0.353(1)	0.355(1)
B/Å^2	0.66	0.58	0.52	0.45
Mn				
B/Å^2	0.24	0.22	0.18	0.28
O1				
z	0.081(1)	0.0	0.0	0.0
B/Å^2	0.71	0.88	0.86	0.94
O2				
x	0.216(1)	0.0	0.0	0.0
z	0.25	0.161(1)	0.156(2)	0.157(1)
B/Å^2	0.98	0.97	0.83	0.88
Magnetic moment/μ_B	1.1(2)	1.5(1)	1.5(2)	1.2(2)
R_{wp}	20.41	18.00	17.47	17.36

Note. The structure was refined in the tetragonal space groups $I4_1/acd$ and $I4/mmm$. The four unique atoms have the following positions: for $I4_1/acd$, (Ca, Sr) (0.0, 0.0, z), Mn (0.0, 0.0, 0.0), O1 (0.0, 0.0, z), and O2 (x, x, 0.25); for $I4/mmm$, (Ca, Sr) (0.0, 0.0, z), Mn (0.0, 0.0, 0.0), O1 (0.0, 0.5, 0.0), and O2 (0.0, 0.0, z).

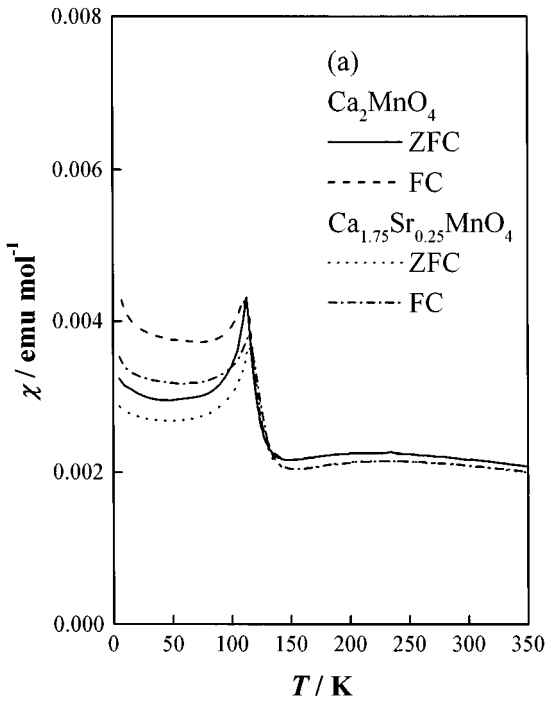

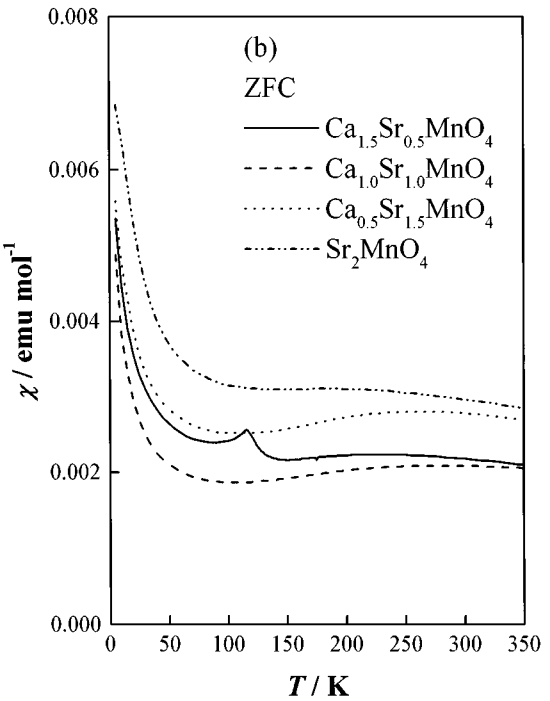

FIG. 4. Magnetic susceptibilities for $Ca_{2-x}Sr_xMnO_4$: (a) $x = 0$ and 0.25 and (b) $x = 0.5$–2.0.

covalency of the Mn^{4+}–O^{2-} bond in the magnetic layers (1).

We have found from the magnetic susceptibility measurement that a ferromagnetic component exists in the magnetic moment of manganese for Ca_2MnO_4 and $Ca_{1.75}Sr_{0.25}MnO_4$ at 10 K. Ferromagnetic Bragg peaks should appear at the same diffraction angles as those of the nuclear Bragg peaks of magnetic atoms. However, reflection intensities due

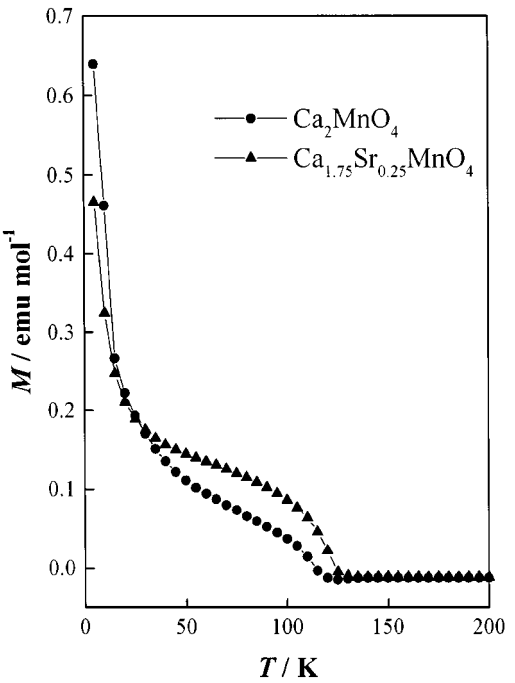

FIG. 5. Remnant magnetization.

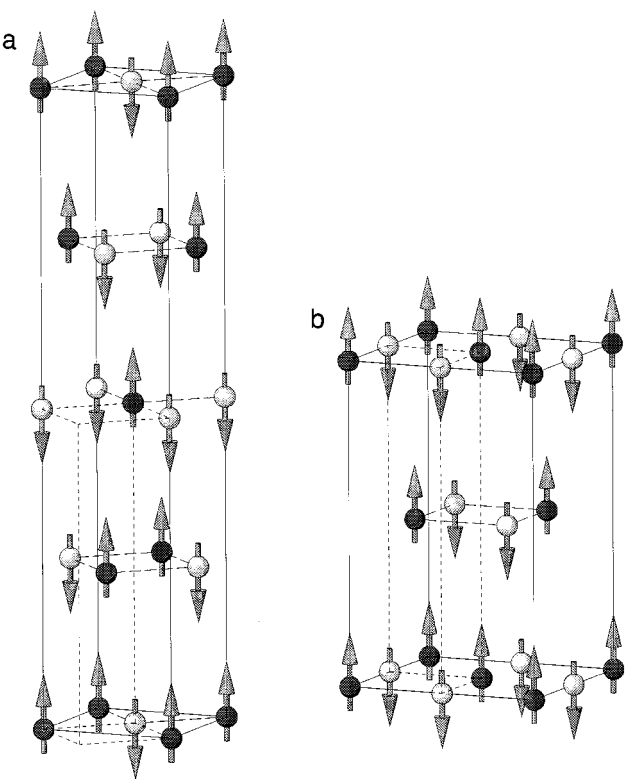

FIG. 6. Magnetic structures of $Ca_{2-x}Sr_xMnO_4$: (a) Ca_2MnO_4 and (b) $Ca_{2-x}Sr_xMnO_4$ with $x = 0.5$–1.5.

to the magnetic diffraction are too small (the ferromagnetic moment is ca. 10^{-4} μ_B/Mn) compared to those due to the nuclear diffraction to estimate the ferromagnetic component from this powder neutron diffraction profile.

SUMMARY

Any solid solution $Ca_{2-x}Sr_xMnO_4$ has a layered perovskite-type structure with the space group $I4_1/acd$ ($x = 0$ and 0.25) or $I4/mmm$ ($x = 0.5$–2.0) and shows antiferromagnetic interaction (at low temperatures). A dramatic difference between ZFC and FC in magnetic susceptibilities found for Ca_2MnO_4 and $Ca_{1.75}Sr_{0.25}MnO_4$ is explained by the Dzyaloshinsky–Moriya interaction.

Magnetic structures of $Ca_{2-x}Sr_xMnO_4$ solid solutions are that the nearest-neighbor Mn^{4+} ions are coupled antiferromagnetically in the (001) planes and that the spins are parallel to the c axis.

REFERENCES

1. J. C. Bouroux, J. L. Soubeyroux, M. Perrin, and G. Le Frem, *J. Solid State Chem.* **38,** 34 (1981).
2. K. Poeppemlmeier, M. E. Leonwicz, and J. M. Longo, *J. Solid State Chem.* **59,** 71 (1985).
3. D. E. Cox, G. Shirane, R. J. Birgeneau, and J. B. MacChesney, *Phys. Rev.* **188,** 930 (1969).
4. J. B. MacChesney, H. J. Williams, J. F. Potter, and R. C. Sherwood, *Phys. Rev.* **164,** 779 (1967).
5. F. Izumi, *in* "The Rietveld Method" (R. A. Young, Ed.), Chap. 13, Oxford University Press, Oxford, 1993.
6. M. K. Crawford, M. A. Subramanian, R. L. Harlow, J. A. Fernandez-Baca, Z. R. Wang, and D. C. Johnston, *Phys. Rev. B* **49,** 9198 (1994).